Experimental Characterisation of Dry and Lubricated Friction on a Newly Developed Rotational Tribometer for Macroscopic Measurements

T. Janssens, F. Al-Bender, H. Van Brussel
K.U.Leuven, Department Mechanical Engineering
Celestijnenlaan 300 B, B-3001, Heverlee, Belgium
e-mail: **Thierry.Janssens@mech.kuleuven.be**

Abstract

A new rotational tribometer is developed which can be used for macroscopic friction measurement and identification. The functional requirements of the tribometer are: (i) accurate displacement and friction force measurement, (ii) normal loading and measurement possibility, both statically and dynamically, and (iii) the possibility of applying arbitrary displacement signals over a large range of magnitude and frequency. These functionalities are decoupled as much as possible based on the principles of precision engineering. Experiments are performed for friction identification, which can be used for control purposes. The tribometer allows experiments in a large range of displacements and velocities, thus allowing various friction characteristics, such as break-away force, pre-sliding hysteresis, friction lag in the sliding regime, stick-slip and limit-cycle oscillations, and the Stribeck behaviour to be measured for one and the same configuration, and under dry or lubricated friction conditions. Such experimental results can be used to validate physically motivated friction models, or to establish or validate empirically motivated friction models, such as used in control applications.

1 Introduction

The characterisation of friction depends on the accuracy of the experimental measurements, and thus the used test setup. Design, qualification and quantification of the used setup are important in the interpretation of the measurement results, which are used to derive the friction characteristics. Owing to its relevance in machines, friction has been measured a numerous amount of times, for many centuries, and it still did not divulge all its secrets. Some measurements are performed on the used machines subject of investigation, and some on specially developed devices, viz. tribometers. The 1989 edition of the Oxford English Dictionary defines a tribometer as an instrument for estimating sliding friction. Thus, the definition of a tribometer is applicable to a broad range of measurement setups. Leonardo da Vinci (1452–1519) was the first to propose an experimental setup for measuring friction, see Figure 1. He measured friction by determining the mass needed for which the block would start moving. At the moment the block starts moving, the friction coefficient is the ratio of the mass of the block and the mass hanging at the cord. The tangential force is applied by gravitation and the use of some kind of pulley. The principle of estimating friction at macroscopic level did not change much during the following half millennium; only the precision of measurement has evolved a great deal.

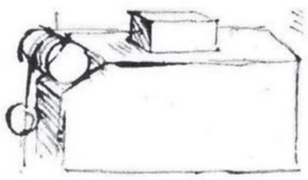

Figure 1: Leonardo da Vinci's sketch of his apparatus for friction experiments (From [2]).

Friction measurements on machines and on some tribometers may be very specific, valid only for those configurations on which they are produced, and may have no general convenience and no general practical use. Frictional behaviour is generally a property of the system and not only of the friction materials in contact [4]. Therefore no single test can reproduce all types of frictional situations. Nevertheless, all friction testing devices, that is tribometers, have several features in common, related to their functional requirements: they provide a way to (i) support two bodies for which friction data is desired, (ii) to apply an arbitrary relative displacement or velocity signal in a controllable way to the contacting bodies, (iii) to apply and measure a load normal to the contact, and (iv) to measure the tangential friction force.

The main subdivision of tribometers is based on the type of displacement which can be applied. The two basic movements, which are used, are: (i) a reciprocating linear movement (e.g. in a sledge configuration) and (ii) a rotational movement (e.g. in a pin-on-disk configuration) [5]. The tribometer described in this paper is of the second type. The main advantages of this type are that it allows high relative velocities and that it can be used when constant sliding velocities are desired. Compared to a linear tribometer, it has an infinite periodic stroke. More specifically, the discussed tribometer is from the disk-on-disk type. It is intended to represent a single contact surface of the type present in a wet clutch of an automatic transmission. Thus it can be categorised as a test rig which can be used for both dry and lubricated friction measurement.

As is usual in experimental friction measurements, only two quantities need to be measured accurately, at constant normal load. These are the friction force and the relative, tangential displacement or velocity between the two objects [5]. As simple as this may seem, it is not always straightforward to measure these quantities dynamically. In many tribological experiments, the friction measurement is complicated because of the vibrational characteristics of the transducer and the structural mechanical system [4]. The static calibration factor of the transducer no longer provides the relation between the strain and friction force when the dynamics of the mechanical force transducer is excited. The ambiguity is that friction and system dynamics cannot be decoupled because the act of measuring friction involves the use of a sensing element with finite compliance. Moreover, inertia effects of the transducer and of the structural mechanical system must be taken into account.

The aim of this paper is to dynamically characterise a newly developed rotational tribometer for macroscopic friction measurement under dry and/or lubricated friction conditions. The experimental results can be used to validate physically motivated friction models or to find or validate empirically motivated friction models, such as those used in control applications. In the case of lubricated conditions the control can be applied in automatic power shifting transmissions.

The structure of the rest of the text is as follows. Section 2 discusses the design and the development of the tribometer. This section is subdivided in the measurement equipment and signal processing and the dynamic evaluation of the tribometer. It discusses the dynamic characterisation, putting focus on the measurement possibilities concerning range, frequency, accuracy, … Section 3 describes the experimental results in the time domain which consist of the break-away force, hysteresis function of the position in the pre-sliding regime, friction lag in the sliding regime, stick slip or dynamic oscillations and Stribeck behaviour. Section 4 contains the conclusion of the text.

2 Design and discussion of the developed tribometer

The design of a setup must take the functional requirements and specifications into account. These are specific for each type of machine or system and, consequently, also for each individual part. The main purpose of our tribometer is to measure the friction force (dry and/or lubricated) occurring between two contacting disks from an automatic transmission with a paper based friction material. Other material and contact combinations are generally also possible. The paper focuses on the measurement of the friction force as a function of the relative tangential motion and normal load for a given specific combination of materials, although this does not necessarily exclude the possibility to use other materials and configurations.

Figure 2 shows an overview picture of the newly developed rotational tribometer. In this picture the following parts can be discerned: (1) shaker (dynamic load), (2) shaker holder, (3) frame, (4) vertical guide ways, (5) cantilever, (6) static load with cantilever, (7) axial bearing, (8) Direct Drive actuator, (9) ball spline bearing, (10) shaft, (11) bellow coupling, (12) tub containing the two friction disks, (13) capacitive displacement sensors (3 off), (14) three ring dynamometers for force and torque measurement, (15) base plate. The normal force is applied with the shaker and the torque is applied with the Direct Drive motor, both through the shaft, which is connected to the upper disk via the bellow coupling. The lower disk is connected to the ring dynamometers.

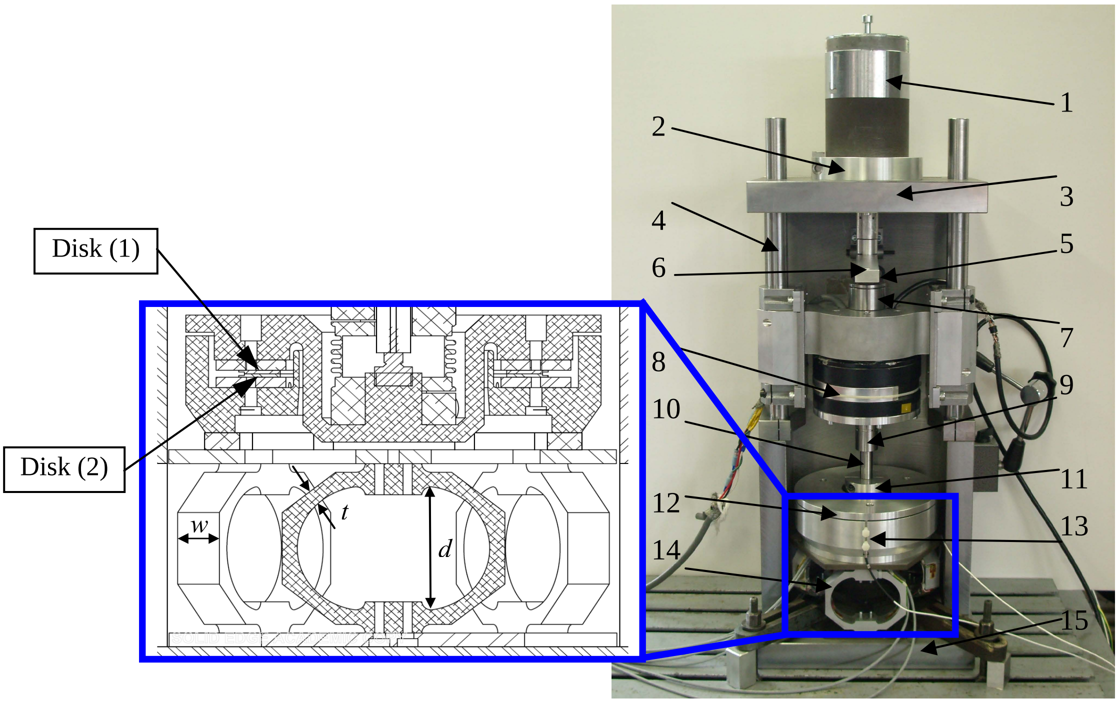

Figure 2: Right: General overview of the rotational tribometer; Left: Cross-section to illustrate the friction disks and ring dynamometers

An added functional requirement to the newly developed rotational tribometer is the ability to measure the normal displacement associated with friction, namely the lift-up effect. This is a relevant effect, certainly when it concerns the normal dynamic effect on the friction behaviour [6]. This is a feature, which is absent on most previously developed tribometers, and so they do not allow the measurement of this lift-up effect.

2.1 Measurement equipment and signal processing

To characterise the friction behaviour between disk 1 and disk 2, see Figure 2, the friction torque, normal force, relative displacement and velocity should be measured dynamically as accurately as possible. This is carried out as follows.

2.1.1 Friction torque and normal force measurement

For the torque and the normal force, a 6-d.o.f. measuring table is designed based on ring dynamometers comprising strain gauges. Three identical ring dynamometers were designed, following the design rules of the state of the art, and manufactured by wire EDM. The main dimensions are: a width w of 25.5 mm, a thickness t of 8 mm and an inner diameter d of 72 mm, see Figure 2. The specifications for one ring dynamometer are as follows. For the normal d.o.f., the maximum allowable force is about 431 N and the resolution is 1/3675 of the full scale. For the tangential d.o.f., the corresponding values are 58.8 N (equivalent to 5 Nm) and 1/1000 of the full scale respectively. In the design, a safety factor of 2 for the maximal allowable stress is used. This is done to make sure the dynamometers do not deform plastically.

Each ring dynamometer is equipped with two full bridges of strain gauges such that each sensor can measure the normal and the tangential force independently. As a bridge amplifier a VISHAY BA 660 strain gauge amplifier with auto-zero is used. The BA 660 is a miniature amplifier, designed to provide signal conditioning for full bridge strain gauge sensors.

2.1.2 Rotational actuation

For the rotational actuation, a Direct Drive Servo Actuator from Dynamserv YOKOGAWA Precision is used with a maximum torque of 15 Nm and a maximum speed of 2.4 r.p.s. The motor has a built-in encoder which is used for the position and velocity measurement. An encoder resolution of 163840 pulses/revolution is used. This actuator is driven by a proportional gain (P) position or velocity controller.

2.1.3 Normal actuation

For the normal actuation, a Philips PR 9270 shaker is used, which can generate a force of 35.7 × I_{eff} [N], with I_{eff} the effective current in amperes. The shaker has a full stroke of 8 mm. This actuator is driven in open loop and has a bandwidth of 0 – 10000 Hz.

2.1.4 Data acquisition

For the data acquisition, a CLP1103 dSPACE system is used. The friction torque measurement is connected to the first three ADC channels which allow a resolution of 16 bit. The other channels have a resolution of 12 bit. The other ADC inputs contain three channels for the normal force, three channels for the normal displacement coming from the LION Precision capacitive sensors, one encoder connection and six digital I/O to reset the torque and the normal force (auto-zero). Two DAC channels are used, one for the motor and one for the shaker.

2.2 Dynamic evaluation of the tribometer

The tribometer system dynamics and its interaction with the friction behaviour play a crucial role in determining the friction force measurement ranges, in regard to amplitude and frequency. Thus, a dynamic identification must be performed in the tangential and in normal directions to obtain the allowable measurement bandwidth. The structural dynamic behaviour of the setup has been optimized during the design phase, the structural resonances being placed at as highest as possible frequencies. The use of a weak P control in a position loop was necessary to get rid of a constant drift due to the velocity control of the motor drive. The results of the identification, the dynamic as well as the frictional, are described further below by several frequency response functions (FRF's). In the tangential excitation case, the torque measured by the dynamometers is considered as being the input and the rotation angle of the motor encoder is considered as being the output. In the normal excitation case, the applied signal to the shaker is considered as being the input, and the normal position of the dynamometric table is considered as being the output. Figure 3 shows a linear schematic representation of the tribometer to illustrate the considered inputs and outputs used for the dynamic identification. The following figures show the measured FRF's using a multisine excitation with different amplitudes, random phase, and a bandwidth of 500 Hz. For each measurement, 4 different multisines, each with different phase, were used and, for each of them 10 periods were taken. By taking the average of the time signal of the 10 measurements, random noise is filtered out. In Figure 4 (A, B and C), the tangential dynamic response is shown given the measured transmitted torque as input and the angular position of the motor coming from the encoder as output.

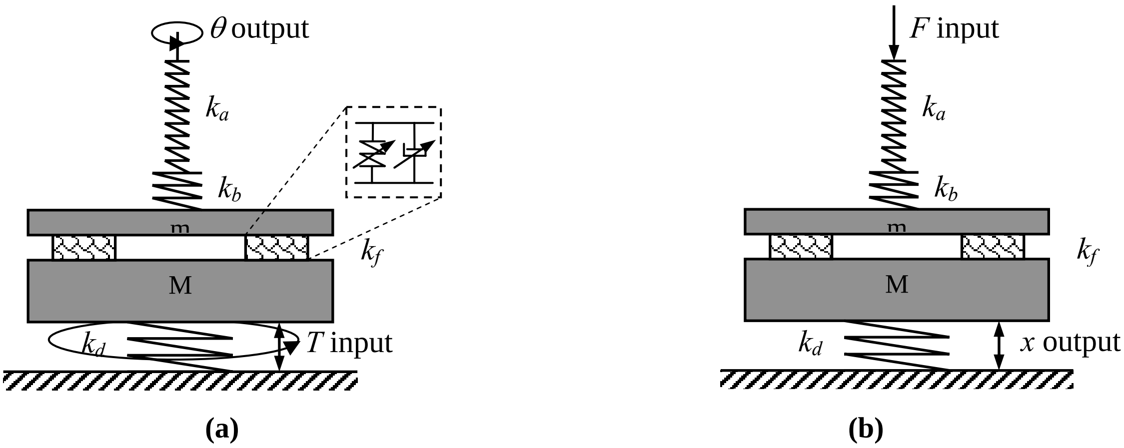

Figure 3: (a): considered input torque *T* and output rotation angle θ for tangential identification, (b): considered input force *F* and output deflection *x* for normal identification, (k_a, k_b, k_f and k_d are the stiffness of the shaft, bellow coupling, friction disk and dynamometers respectively), k_f is represented as a variable spring/damper function of the amplitude and frequency of the deflection and of the normal load

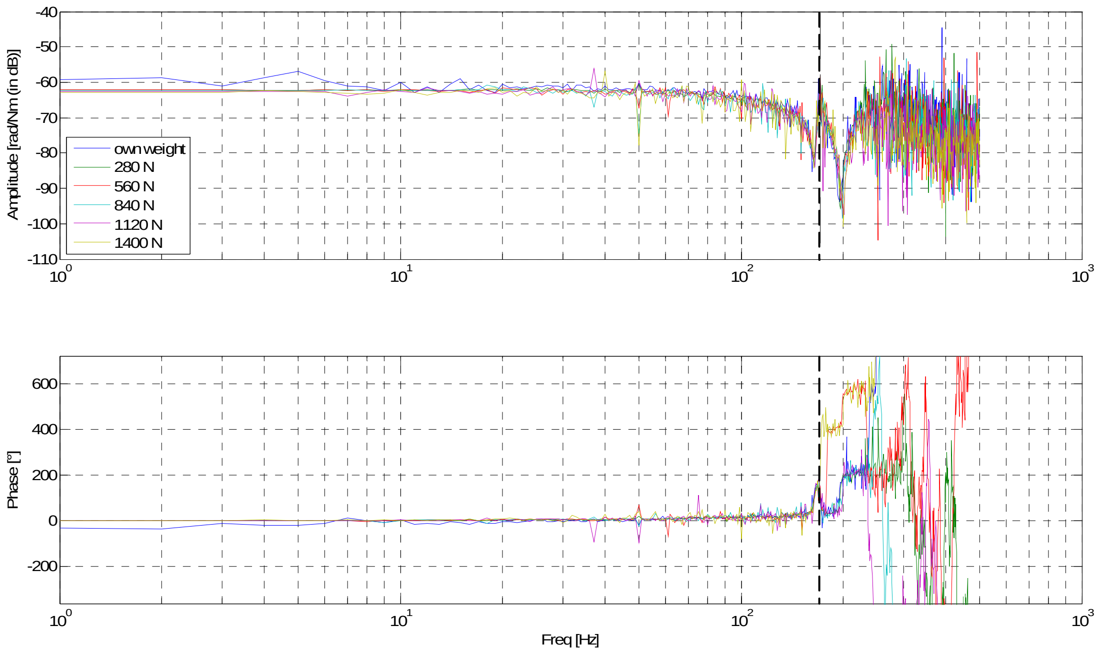

Figure 4.A: Tangential FRF for A=0.015 V

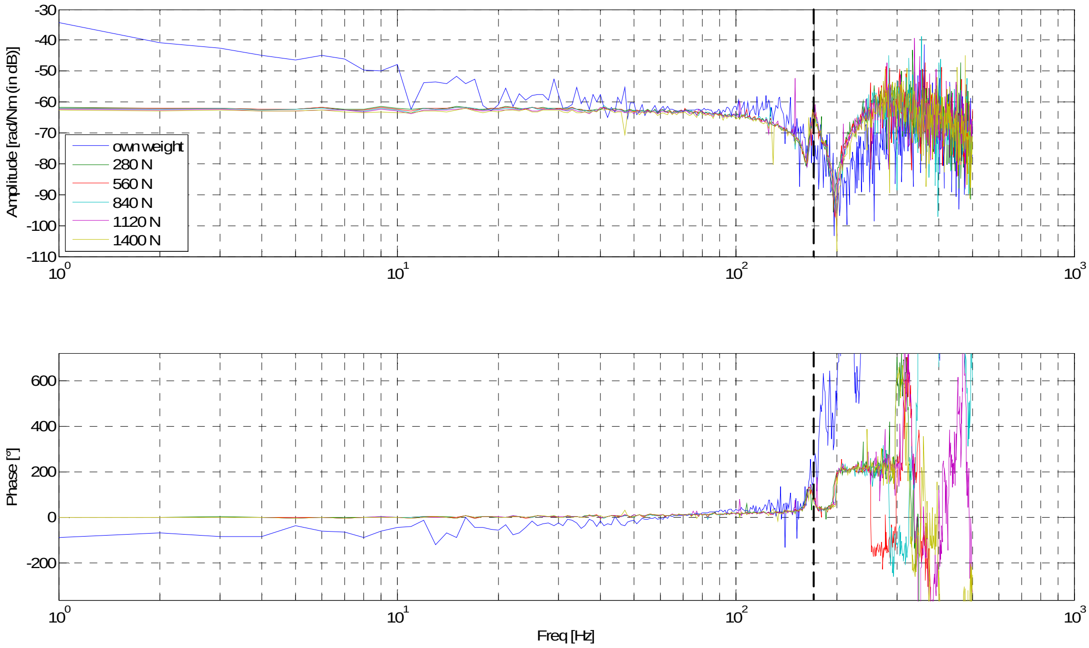

Figure 4.B: Tangential FRF for A=0.03 V

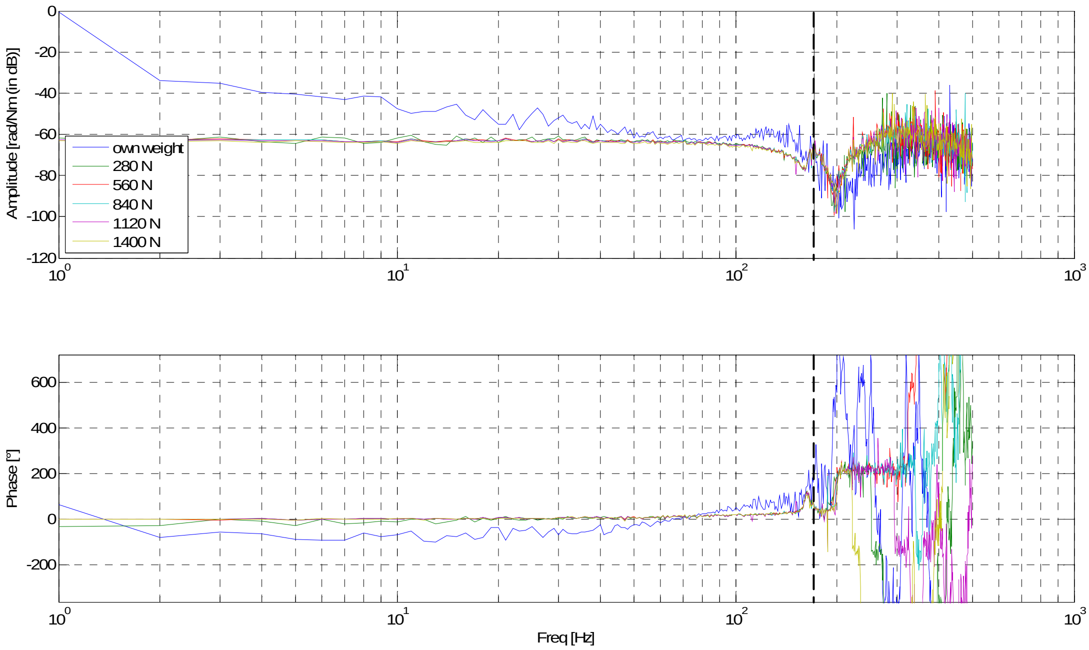

Figure 4.C: Tangential FRF for A=0.06 V

This tangential identification has been performed for three different amplitudes of the multisine excitation, namely for A = 0.015 V, A = 0.03 V and A = 0.06 V, and for different normal preloads.

As can be seen in the FRF's the tangential dynamic behaviour is relatively linear when high normal loads are applied. When the normal load is not high enough, that is, at a normal load which consists only of the weight of the driving parts (6, 7, 10, 11 and the upper disk, which amount to about 58 N), a nonlinear effect can be observed. The slope of the amplitude at low frequencies goes from 0 dB/decade towards -40 dB/decade for increasing amplitudes of excitation, corresponding to a mass-line. This behaviour, which arises from the hysteresis characteristics of the frictional contact, is treated exhaustively in [7]. In particular, the irregularities observed in the FRF pertaining to the lowest preload arise from the sensitivity of the response to small amplitude variations; a jump-like phenomenon [7]. The hysteresis nature of the contact will become apparent in the section on friction identification further below. In the three previous plots a dashed vertical line indicates the frequency at which the first tangential resonance frequency lies; i.e. somewhere around 170 Hz.

The normal dynamic response has also been identified, in a similar way to the tangential response. In Figure 5, the normal dynamic response is shown, where the applied signal to the shaker is the input and the normal force, measured in the dynamometers by strain gauges, is the output. This output force is proportional to the normal displacement in the dynamometers.

Also in this plot a dashed vertical line indicates the frequency at which the first normal resonance frequency, pertaining to lowest preload, is lying, namely at about 186 Hz. One can observe a shift in the first eigenfrequency to the right and a change in global dynamic response with rising preload, seen as a merge of the consecutive poles and zeros. This behaviour is due to the increase in the stiffness of the contact, it being essentially a Hertzian contact, with increased loading. At low preloads, one can also observe multiple eigenfrequencies, whereas with high preload there are only two, one at the shifted first eigenfrequency and one at about 288 Hz, due to the merge.

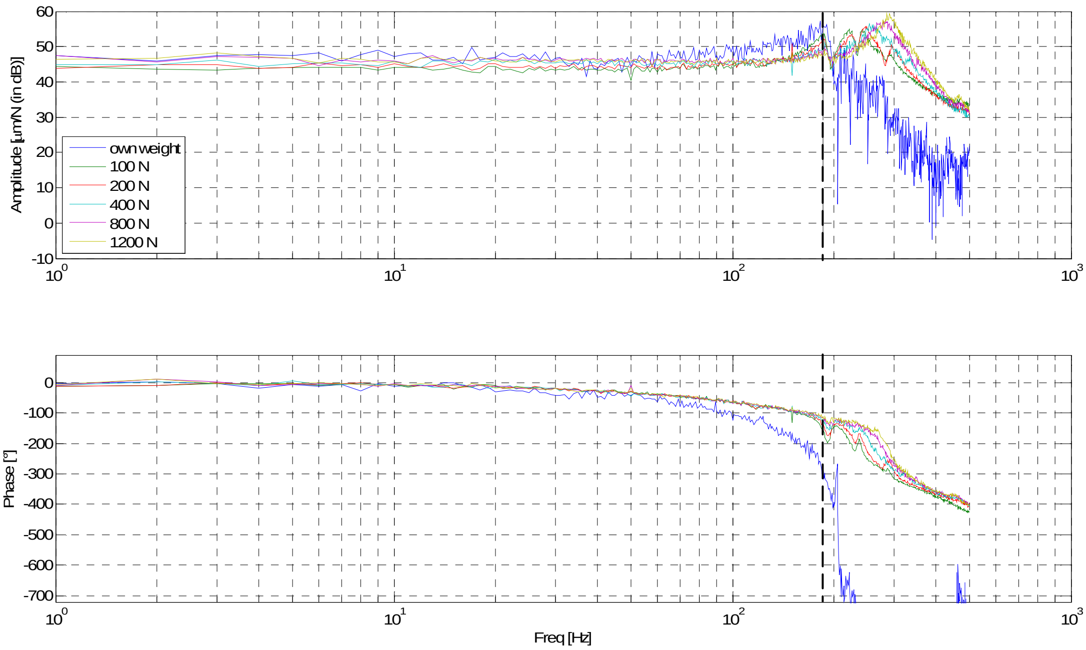

Figure 5: Normal FRF (deflection of dynamometers/shaker force)

In order to ascertain the nonlinear, friction hysteresis effect on the FRF, the case of lowest preload is further examined, presently with increasing amplitude of excitation. Figure 6 shows the FRF for this identification. The amplitude of the FRF increases with amplitude of excitation, to approach a virtual mass-line. This identification was also performed with a stepped sine, as in [7], and resulted in a similar response.

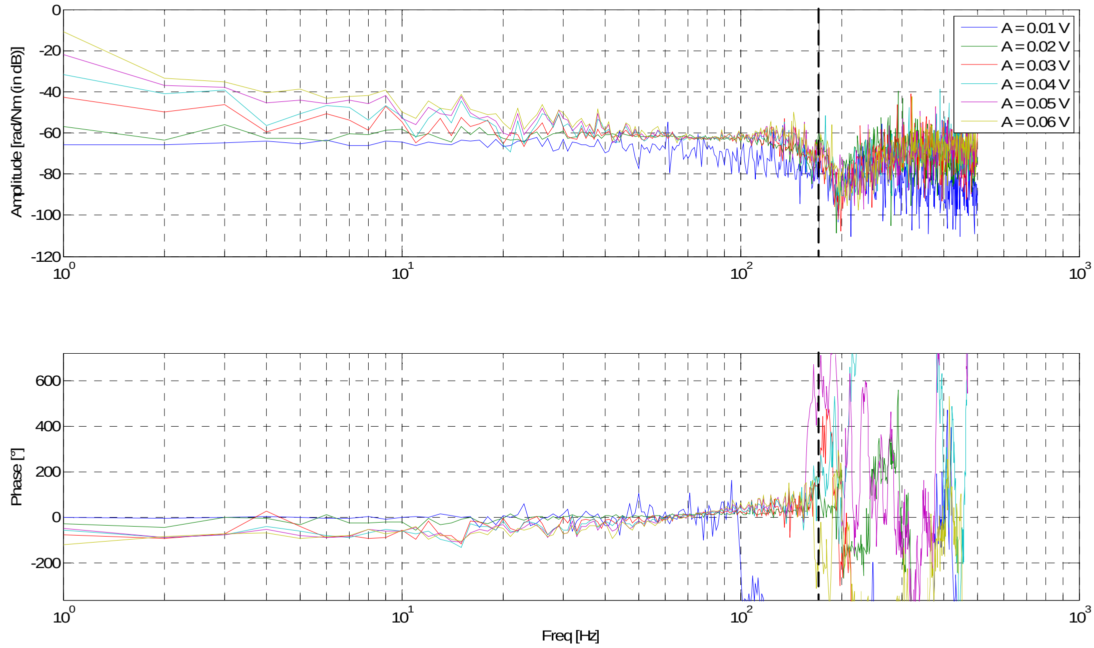

Figure 6: Nonlinear tangential FRF (effect of friction)

Compared to the four preceding FRF's, this one is much noisier. This is due to the lower signal to noise ratio, which is in turn dictated by the relatively low stiffness in the contact. This FRF was performed in a non-preloaded situation, with the only normal load the own weight of the friction plate and the driving ball spline and shaft. As mentioned earlier the slope of the amplitude at low frequencies goes from 0 dB/decade to -40 dB/decade for increasing amplitudes of excitation. The bounds, within which this measured FRF will lie, are the mass-line (for high excitation) and the mass-spring curve (for low excitation).

The occurrence of an anti resonance before the resonance in the tangential FRF's should also be mentioned. This result can be due to a particular component in the setup which behaves as an energy sink at a frequency lower then the first eigenfrequency.

Modal analysis bases on hammer excitation revealed some extra modes within this bandwidth. This hammer excitation was performed on the measuring table composed of the lower friction disk and the three ring dynamometers. Most of these identified modes are tilting modes and the main normal and tangential mode where also clearly visible. The torsional mode of the measuring table has a frequency of about 222 Hz as compared to 170 Hz when the friction surfaces are in contact and preloaded.

A dynamic identification is performed in the tangential and in normal directions to obtain the allowable measurement bandwidth. Based on the previous results and FRF's this can be determined up to a bandwidth of 100 Hz. This bandwidth is used to filter the experimental results in time domain.

3 Experimental results in the time domain

The tribometer allows experiments in a large range of displacements/velocities, thus allowing numerous friction characteristics to be observed on one and the same configuration and under dry and/or lubricated friction conditions. Typical friction characteristics are: break-away (or the static friction) force, hysteresis as a function of the position in the pre-sliding regime, friction lag in the sliding regime, stick-slip or dynamic oscillations, and Stribeck behaviour as described in literature [[1], [3]]. These experimental results can be used to validate physically motivated friction models or to formulate or validate empirically motivated friction models, which are often used for control purposes, e.g. to compensate friction in the form of stick-slip, dynamic oscillations or other self induced vibrations such as shudder [8].

The friction force as a function of the relative displacement and normal load is given for a specific combination of materials under investigation, namely a paper based clutch disk on a steel counter disk. Here the dynamic friction force for different combinations of materials is not relevant. This does not necessarily exclude the possibility of using different materials and configurations. The results discussed in the next sections are all obtained after running-in the contact, to ensure as uniform subsequent behaviour as possible. It should be mentioned here that since a rotational tribometer is used, position dependent friction, such as periodic behaviour due to the profile of the disks, may easily occur in the measurements.

3.1 Break-away force

The force necessary to initiate total slip, or gross sliding, can be determined. The maximum force which occurs in this initiation is called the break-away force [[1], [9]]. In the case of a rotational tribometer the motion is circular and then we talk about the break-away torque. The experiment to measure the break-away torque is performed for different accelerations, from stick, under a normal load of 280 N. These different accelerations are applied to the system, and these result in different increasing torques due to stick in the friction contact. The break-away torque is here defined as the maximum friction torque during the transition from pre-sliding (stick) to gross sliding regime.

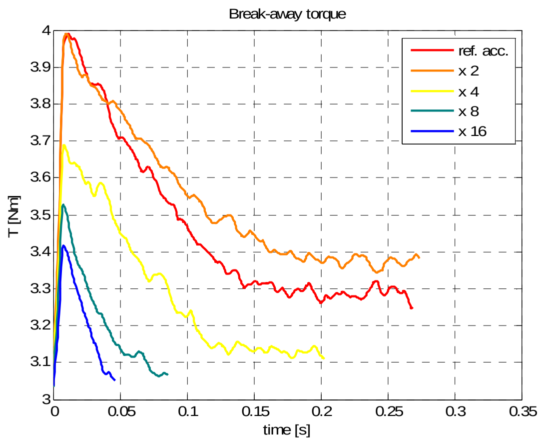

Figure 7: Break-away torque for different applied accelerations with a normal load of 280 N

One may use this definition of break-away force, as being equivalent to the static friction. But as can be seen in Figure 7, due to the dependence on the application rate, several values for the static friction can be found for one and the same normal load. For the lowest acceleration the highest maximal torque is attained and this maximum decreases with increasing acceleration [[1], [10]]. The maxima can be compared with the friction torque at zero velocity with the same applied load, as can be seen in Figure 10.

3.2 Pre-sliding regime

The pre-sliding regime is defined as the region in which the adhesive forces at asperity contacts are dominant such that the friction force appears to be a function of the displacement [[11], [12], [13]]. To investigate the friction behaviour in the pre-sliding regime, a desired position signal is applied to the system using a proportional controller. This desired trajectory consists of a saw tooth position in function of time, with maximum amplitude of about 0.0003 rad, having two reversal points with smaller amplitude. The amplitude of the signal is chosen such that the actual displacement remains within the pre-sliding regime.

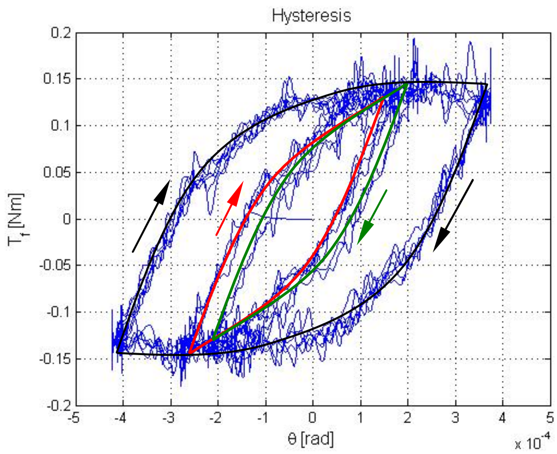

Figure 8: Hysteresis in pre-sliding regime with non-local memory effect

The resultant friction force, from this pre-sliding experiment, in function of displacement, can be seen in Figure 8. A hysteresis behaviour with non-local memory is defined as an input-output relationship for which the output at any time instant not only depends on the output at some time instant in the past and the input since then, but also on the past extreme values of the input or the output [14]. This can be perceived in the two inner loops in the hysteresis in Figure 8, see also [7] for details of the hysteresis function construction and modelling.

3.3 Friction lag in sliding regime

To investigate the behaviour in the transition from pre-sliding to sliding and vice-versa, a sinusoidal position command trajectory is applied to the system, with an amplitude of 0.06 rad for three different frequencies.

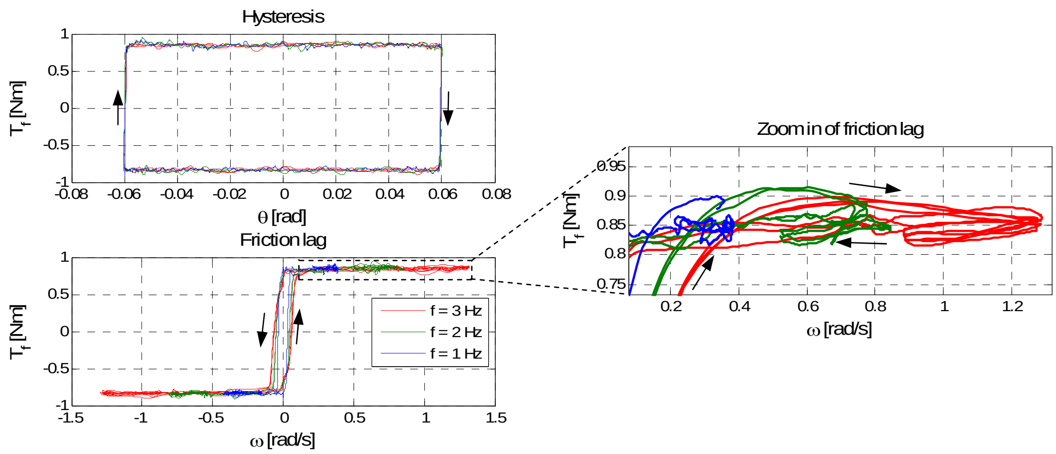

Figure 9: Left: Hysteresis and corresponding friction lag: blue f = 1 Hz, green f = 2 Hz, red f = 3 Hz, Right: zoom in of friction lag

The measured velocity is not a pure sinusoidal signal due to the effect of friction, as can be seen at velocity reversal in Figure 9. This demonstrates the paradox of a tribometer: the controller which tries to impose the desired displacement signal is limited due to nonlinear disturbances. The main disturbance signal comes from the friction interaction. We can see a higher friction force during acceleration compared to the friction force during deceleration. This phenomenon is called friction lag or hysteresis in the sliding regime. The Stribeck curve (see section 3.4), should intersect the loop formed by the friction force belonging to increasing and decreasing velocity during sliding. The measurement of this Stribeck curve is not trivial due to the stick-slip property of friction (see section 3.5). [1] and [15] also measured a friction lag behaviour for oscillatory rubbing contacts.

3.4 Stribeck behaviour

In the static regime the friction force is independent of the velocity. As soon as the break-away force is exceeded and the object starts to slide, the friction force generally drops to a lower value. It was found by Stribeck that the velocity dependence is continuous [3]. The typical drop (rise) in the Stribeck curve, which represents the friction force in function of velocity, for positive (negative) velocities is called Stribeck effect. Figure 10 shows the Stribeck curve for a velocity range up to 0.6 rad/s, for three different applied loads. For all the experiments the Stribeck effect is clearly visible and the viscous effect can also be seen as the rising part of the Stribeck curve, see Figure 10. The Stribeck curve is the combination of the Stribeck effect and the viscous effect. For the lowest applied load the position dependence of the friction force strongly affects the shape of the Stribeck curve and perceived as a fluctuation in the friction force.

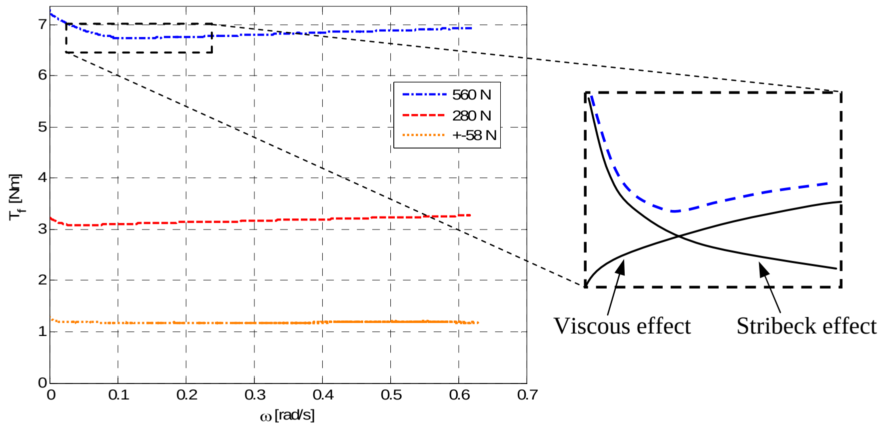

Figure 10: Stribeck curve for different loads, and its components

3.5 Stick-slip motion

To measure stick-slip motion a constant desired velocity is applied to the system. A necessary condition to induce stick-slip is a decreasing friction force for a rising velocity. That is, the dynamic friction force is lower then the static friction force. This phenomenon is known as the Stribeck effect, see section 3.4. Stick-slip can be described as follows. The critical velocity is defined as the maximum driving velocity below which stick–slip will occur [16]. When a constant driving velocity, lower than the critical velocity, is applied to the upper disk, the disk will initially stick and the friction force will build up until it reaches a maximum equal to the break-away force. Once this maximum is reached, the disk will start slipping and due to the decreasing friction force it will accelerate. After this acceleration the system will decelerate until it reaches again zero velocity due to the actuating stiffness. At this moment, the cycle can start again. If the moving body never reaches zero velocity, it will never stick but it can still exhibit an oscillatory behaviour around the desired velocity. This motion is referred to as dynamic oscillations or limit cycle hunting, but in literature this is also often called stick-slip motion [[17], [18]].

Figure 11 and Figure 12 show the stick-slip behaviour for two different applied loads and five command velocities (ω_1 = 4, ω_2 = 5.98, ω_3 = 9.44, ω_4 = 13.74, ω_5 = 20 [$\times 10^{-3}$ rad/s]). In these figures the velocity is rising from top to bottom and as can be seen in Figure 11, the velocity apparently reaches a value higher than the critical velocity because the stick-slip phenomenon does not occur anymore. For the same applied velocity at 87 N stick-slip still occurs.

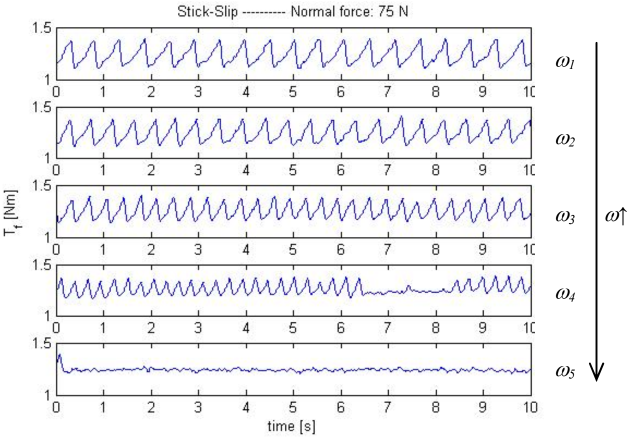

Figure 11: Stick-Slip with 75 N normal force

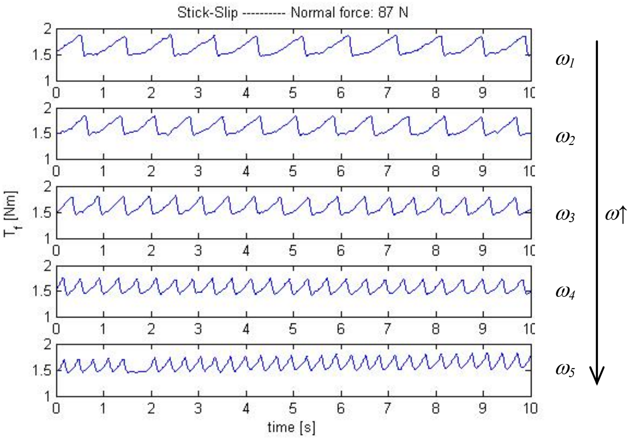

Figure 12: Stick-Slip with 87 N normal force

We may conclude that the higher the normal load, the higher the critical velocity for which stick-slip still occurs. This is supported by the fact that the velocity corresponding to the minimum point in the Stribeck curve shifts up with increasing preload, see Figure 10.

4 Conclusions

Friction and system dynamics cannot be decoupled because the act of measuring friction involves the use of a sensing element with finite compliance. Moreover, inertia effects of the transducer and of the structural mechanical system must be taken into account, they are never infinitely stiff. It appears that friction between two contacting bodies is not strictly a function of the materials in contact and the contact conditions, but also of the measurement approach. After the dynamic evaluation of the developed tribometer, different friction experiments in time domain are carried out. This setup allows us to investigate different friction phenomena, such as break-away, the pre-sliding and sliding behaviour, the transition between regimes, stick slip motion and Stribeck behaviour. The next step will be to investigate these friction phenomena in lubricated conditions. The results of these experiments can be used as a validation for friction models.

Acknowledgements

This research is funded by the IWT, the Institute for the Promotion of Innovation by Science and Technology in Flanders, Belgium, grant SB-53043.

References

[1] Lampaert V., Al-Bender F., Swevers J., *Experimental Characterisation of Dry Friction at Low Velocities on a Developed Tribometer Setup for Macroscopic Measurements*, Tribology Letters, 16(1-2)95-105, (2003)

[2] Dowson D., *History of Tribology* (2nd ed.), Longman Ltd., London, (1998)

[3] Stribeck R., *Die wesentlichen Eigenschaften der Gleit- und Rollenlager – The key qualities of sliding and roller bearings*, Zeitschrift des Vereines Deutscher Ingenieure, 46(38,39):1342–1348, 1432–1437, (1902)

[4] Aronov V., D'Sousa A., Kalpakjian S., Shareef I., *Interactions Among Friction, Wear, and System Stiffness -part2: Vibrations Induced by Dry Friction*, ASME Journal of Tribology, 106,59-64, (1984)

[5] Blau P.J., *Friction Science and Technology*, Marcel Dekker Inc., New York, (1996)

[6] Tolstoi D.M., *Significance of the normal degree of freedom and natural normal vibrations in contact friction*, Wear 10, 199–213, (1967)

[7] Al-Bender F., Symens W., Swevers J., Van Brussel H., *Theoretical analysis of the dynamic behavior of hysteresis elements in mechanical systems*, International Journal of Non-linear Mechanics 39, 1721-1735, (2004)

[8] Kugimiya T., Yoshimura N., Mitsui J., *Tribology of automatic transmission fluid*, Tribology Letters, Volume 5, Number 1, pp. 49-56(8), (1998)

[9] Berger E. J., *Friction modeling for dynamic system simulation*, Appl. Mech. Rev. 55, 535 (2002)

[10] Johannes V. I., Green M. A., Brockley C. A., *The role of the rate of application of the tangential force in determining the static friction coefficient*, Wear, 24,381-385(1973)

[11] Prajogo T., *Experimental study of pre-rolling friction for motion-reversal error compensation on machine tool drive systems*, Dept. Werktuigkunde Katholieke Universiteit Leuven, Leuven, (1999)

[12] Armstrong-Hélouvry B., Dupont P., Canudas De Wit C., *A survey of models, Analysis Tools and Compensation Methods for the Control of Machines with Friction*, Automatica, 30(7),1083-1138, (1994)

[13] Swevers J., Al-Bender F., Ganseman C., Prajogo T., *An integrated friction model structure with improved presliding behaviour for accurate friction compensation*, IEEE, Trans. on Automatic Control, 45,675–686, (2000)

[14] Mayergoyz I. D., *Mathematical models of hysteresis*, Springer-Verlag, New-York, (1991)

[15] Kappagantu R. V., Feeny B. F., *Proper Orthogonal Modes of a Beam With Frictional Excitation, Series on Stability, Vibration and Control of Systems: Series B*, 14,167-172, (1998)

[16] Armstrong-Hélouvry B., *Stick-Slip Arising from Stribeck Friction*, Proc. 1990 Inter. Conf. on Robotics and Automation, pp. 1377-82, (1990)

[17] Hess D. P., Soom A., *Friction at a lubricated line contact operating at oscillating sliding velocities*, ASME Journal of Tribology, 112 (1), 147-52, (1990)

[18] Holgerson M., Lundberg J., *Engagement Behaviour of a Paper-Based Wet Clutch Part 2: Influence of Temperature*, Proceedings of the I MECH E Part D Journal of Automobile Engineering, Volume 213, Number 5, pp. 449-455(7), (1999)